Protein scaffold-based multimerization of soluble ACE2 efficiently blocks SARS-CoV-2 infection *in vitro*

Alisan Kayabolen[1,*], Ugur Akcan[1,4], Dogancan Ozturan[1,4], Ehsan Sarayloo[1], Elif Nurtop[2], Berna Ozer[2], Gizem Nur Sahin[1], Ozlem Dogan[2], Nathan Lack[1,3], Mehmet Kaya[1], Cem Albayrak[1], Fusun Can[2], Ihsan Solaroglu[1,*], Tugba Bagci-Onder[1,*]

[1] Koç University Research Center for Translational Medicine (KUTTAM), Koç University, Istanbul, Turkey

[2] Koç University IşBank Research Center for Infectious Diseases (KUISCID), Istanbul, Turkey

[3] Vancouver Prostate Centre, University of British Columbia, Vancouver, Canada

[4] These authors contributed equally

* Corresponding authors

Koç University School of Medicine,

Koç University Research Center for Translational Medicine

Rumelifeneri Yolu, 34450, Sariyer, Istanbul, TURKEY

E-mail: tuonder@ku.edu.tr,

Running title: Multimeric sACE2 blocks SARS-CoV-2 infection

Word count: 2379

Abstract

Soluble ACE2 (sACE2) decoy receptors are promising agents to inhibit SARS-CoV-2 as they are not affected by common escape mutations in viral proteins. However, their success may be limited by their relatively poor potency. To address these challenges, we developed a highly active multimeric sACE2 decoy receptor via a SunTag system that could neutralize both pseudoviruses bearing SARS-CoV-2 spike protein and SARS-CoV-2 clinical isolates. This fusion protein demonstrated a neutralization efficiency nearly 250-fold greater than monomeric sACE2. SunTag in combination with a more potent version of sACE2 achieved near complete neutralization at a sub-nanomolar range, which is comparable with clinical monoclonal antibodies. We demonstrate that this activity is due to greater occupancy of the multimeric decoy receptors on Spike protein as compared to monomeric sACE2. Overall, these highly potent multimeric sACE2 decoy receptors offer a promising treatment approach against SARS-CoV-2 infections including its novel variants.

Coronavirus disease 2019 (COVID-19) is a disease caused by severe acute respiratory syndrome coronavirus 2 (SARS-CoV-2) (1). It was firstly diagnosed in late 2019 in Wuhan, China (2) and has since spread over the globe, leading the WHO to declare a pandemic on March 11, 2020 (3). As of January 2, 2021, there have been more than 84 million reported cases of COVID-19, that have caused more than 1.8 million reported deaths worldwide (4). Several vaccine candidates have been developed in a remarkably short period of time and shown to be highly effective in phase III clinical trials (5–8). Despite these promising results, producing vaccines in sufficient amounts and distributing them worldwide to stop the disease is likely to be a very long and challenging process. There is also no evidence as of yet that the available vaccines will provide long-term protection, or protection against potential novel variants of SARS-CoV-2. Therefore, novel drugs targeting SARS-CoV-2 specifically, and all of its possible variants, are needed to provide a reliable and effective therapy for this disease.

Currently, viral replication inhibitors such as remdesivir or favipiravir, which were initially developed for Ebola or influenza, respectively, are regarded as a standard of care in the treatment of COVID-19 (9, 10). However, clinical trials indicated little or no effect of these drugs especially for patients with severe symptoms (11, 12). Although there are numerous ongoing studies and clinical trials, drugs specifically targeting SARS-CoV-2 have not been identified.

To date, the only cell surface receptor shown to be responsible for SARS-CoV-2 infection is Angiotensin-converting enzyme 2 (ACE2) (13–18). Upon binding to this protein, SARS-CoV-2 enters cells via cleavage of its spike glycoprotein by either membrane proteases such as TMPRSS2, or endosomal proteases such as cathepsin B/L (17). Camostat mesylate, which inhibits TMPRSS2, and E64d, which inhibits cathepsin B/L proteases, were also found to be effective to neutralize virus (17). Accordingly, inhibitions of these pathways were offered to block virus entry, and their efficacy is being tested in clinical trials (19). Natural or synthetic antibodies against ACE2 (20–25) or SARS-CoV-2 Spike (26), have been developed to prevent SARS-CoV-2 Spike binding to cellular ACE2. However, many viruses including SARS-CoV-2 were shown to acquire escape mutations under such evolutionary pressure (27). Therefore, soluble ACE2 and its more potent mutant forms have been proposed as alternatives to neutralizing antibodies (28–30) as the virus cannot develop resistance without compromising cell entry. Soluble ACE2 was shown to inhibit SARS-CoV-2 infection in cell culture experiments (31), *in vitro* human organoids (31), and recently on a COVID-19 patient with severe symptoms (32). However, sACE2 is not evolved to be the natural receptor of SARS-CoV-2 spike protein. For this reason, it has to be used in high concentrations in order to achieve sufficient levels of neutralization.

To address this challenge, we aimed to increase neutralization efficiency by fusing alternative protein domains with soluble ACE2 (sACE2) (**Figure 1A** and **Figure S1**). We explored several different strategies including SARS-CoV-2 co-targeting and protein multimerization. In these fusion proteins, we utilized either the wild type sACE2(WT), or its mutant form, sACE2(v1), which binds SARS-CoV-2 Spike with higher affinity (28). For our co-targeting proteins, we fused the extracellular domains of PAI1/*SERPINE1* or A1AT/*SERPINA1*, known TMPRSS2 inhibitors (33), with the C terminus of sACE2 via a GS rich linker (**Figure 1A**). Similarly, we fused the extracellular domain of cystatin C/*CST3*, which was shown to inhibit cathepsin B/L in the endosomal pathway (34, 35), with sACE2 (**Figure 1A**). Finally, we hypothesized that multimerization of sACE2 would more closely mimic the physiological protein concentrations found on cells and could potentially block viral cell entry more effectively than the soluble sACE2. To test this, we utilized a multimerization system called SunTag, which was originally developed for signal amplification in fluorescence imaging (36). This system consists of two tags; a small GCN4 domain, a transcription factor found in yeast, and a scFv domain that is specific to the GCN4 tag (**Figure 1A**). In the original SunTag study, the authors had used up to 24xGCN4 tags

to allow recruitment of 24 copies of GFP. However, as sACE2 is significantly larger than GFP, we instead used a 5xGCN4 tag, which had been incorporated in a dCas9-based gene activation system to recruit 5 copies of TET1, a similarly sized protein to sACE2 (37). In our constructs, we separately incorporated both the 5xGCN4 and scFv tags to sACE2. Using both components together, we expected that sACE2 would be multimerized with these tags and bind to the multiple Spike proteins. Therefore, achieving higher neutralization levels would be possible by increasing the sACE2 presence on the SARS-CoV-2 virion.

To test the neutralization efficiencies of designed constructs in a BSL-2 level laboratory, we generated lentiviral-based pseudotyped viruses containing a SARS-CoV-2 Spike glycoprotein and a GFP or luciferase transfer plasmids to measure cellular infection. These Spike-bearing pseudoviruses were then used to infect HEK293T cells transiently expressing ACE2 and TMPRSS2. In parallel with the findings of Hoffmann et al. (2020) (17), cells co-expressing both ACE2 and TMPRSS2, were infected much more efficiently by Spike-bearing pseudoviruses, compared to cells expressing them individually (**Figure S2A and S2C**). This phenotype was also confirmed with fLuc packaged Spike-bearing pseudoviruses (**Figure S2E**). Interestingly, the relative infection efficiency was not significantly different with VSVG-bearing pseudoviruses (**Figure S2B and S2D**). We also compared two different codon optimized Spike constructs when generating pseudoviruses, including the full-length version or 18-aa truncated version. The infection rate was nearly 6 times higher with the 18-aa truncated Spike (**Figure S2C**). Demonstrating the specificity of this model, pseudovirus infection was blocked with recombinant ACE2 protein (**Figure S2F**). Encouraged by these results, ACE2 and TMPRSS2 co-expressing cells, and pseudoviruses bearing 18-aa truncated Spike were used for further experiments.

Following the cloning of our fusion proteins, we expressed them in HEK293T cells. As all fused proteins have sACE2 in their N termini, they were secreted into the culture media. Assuming a similar expression for all constructs, we collected serum-free conditioned media (CM) and performed a small screen to test for pseudovirus neutralization (**Figure 1B**). Cell infection of the GFP encoding pseudoviruses were initially confirmed by microscopy and then quantified by a fluorescent plate reader (**Figure S3A**), while fLuc-encoding pseudoviruses were quantified by a luminescence assay (**Figure S3C**). From this initial screen, we observed that sACE2(WT) did not significantly impact pseudovirus neutralization. However, similar to findings of Chan et al. (28,

30), sACE2(v1) including H34A, T92Q, Q325P, A386L mutations, could significantly inhibit the cell entry of pseudoviruses. The CST3 and A1AT fusions slightly increased the effects of both sACE2(WT) and sACE2(v1). As they were not strongly effective individually (**Figure S3B**), we conclude that fusion with sACE2 might enhance their activity by bringing them closer to their target enzymes. However, the most striking results were obtained with the SunTag system, particularly when fused with the sACE2(WT). Crude CMs from both sACE2(WT)-SunTag and sACE2(v1)-SunTag almost completely blocked pseudovirus infection (**Figure 1C**). As the individual components, sACE2-5xGCN4 and sACE2-scFvGCN4, had similar activity to the untagged sACE2, the pseudovirus neutralization occurred through multimerization of sACE2. Moreover, this result is compatible with the recent studies indicating natural dimerization (28) or engineered trimerization (29) of sACE2 increased the Spike binding affinity and neutralization capacity.

As a comparison, we included small molecule inhibitors of TMPRSS2 and Cathepsin B/L (Camostat mesylate and E64d) (17) in our pseudotyped virus neutralization assay. These inhibitors were effective in the micromolar concentration range as expected. However even at the highest concentrations (100 µM), they were not as potent as sACE2(WT)-SunTag or sACE2(v1)-SunTag CM in inhibiting virus entry, attesting to their superior efficacy.

We observed that both sACE2(WT)-SunTag and sACE2(v1)-SunTag CMs blocked more than 90% of pseudovirus infection. To be able to compare the dosage dependency, we next performed limiting dilution assay (**Figure 2A**). sACE2v2.4(732) was also added to the dilution assay, as it was shown to be highly potent against Spike, because of the point mutations and the natural dimerization domain (28, 30). As expected, without dilution, sACE2v2.4(732) was more effective than the sACE2(WT) or sACE2(v1) and similar with WT-SunTag and v1-SunTag. However, even after 5x dilution, it was clear that both WT-SunTag and v1-SunTag neutralized pseudoviruses were much better than the others and were still effective after 50x dilution (**Figure 2A**).

To preclude non-specific effects from other secreted proteins present in the conditioned media, we generated recombinant proteins *in vitro* using 8xHis tagged WT, WT-SunTag, v1, and v1-SunTag ACE2 (**Figure 2B**) followed by fPLC purification. *In vitro* generated monomeric sACE2(WT), was shown to have comparable activity (IC_{50} = 358 ± 114 nM) to commercially available

recombinant sACE2 (IC_{50} = 275 ± 78 nM) (**Figure S2F**). In contrast, the sACE2(WT)-SunTag had more than 250-fold increased neutralization capacity (IC_{50} = 1.35 ± 0.24 nM) than the monomeric sACE2(WT). Further, similar to our earlier results, the purified sACE2(v1)-SunTag was the most efficient system, with a sub-nanomolar median (IC_{50} = 0.30 ± 0.07 nM) inhibitory concentration (**Figure 2C**).

To extend our findings from the pseudotyped virus system to a bona fide SARS-CoV-2 infection system, we carried out neutralization assays with clinical isolates of SARS-CoV-2 in BSL-3 laboratory. Accordingly, both sACE2(WT)-SunTag and sACE2(v1)-SunTag blocked SARS-CoV-2 entry to Vero-CCL81 cells much more efficiently than their untagged counterparts **(Figure 3A and Figure S4**). sACE2(WT)-SunTag neutralized 10^5 pfu/ml SARS-CoV-2 with an IC_{50} value of 2.09 ± 0.45 nM (**Figure 3A**) and 10^3 pfu/ml SARS-CoV-2 were neutralized with a sub-nanomolar IC_{50} value (0.15 ± 0.04 nM) (**Figure 3A**). This result indicates that the addition of SunTag allows the use of wild type ACE2 as a highly efficient trap for SARS-CoV-2 neutralization, which prevents any possibility of escape mutations. Similarly, sACE2(v1)-SunTag neutralized SARS-CoV-2 with a sub-nanomolar median inhibitory concentration in both 10^5 pfu/ml (IC_{50} = 0.84 ± 0.05 nM) and 10^3 pfu/ml titers (IC_{50} = 0.06 ± 0.01 nM) (**Figure 3A**). These neutralization values are better than or comparable to several monoclonal antibodies developed in recent studies (20).

From these results, we proposed that the SunTag system blocks SARS-CoV-2 by recruiting multiple sACE2 more efficiently around the virion (**Figure 4B**). To test this hypothesis, we performed a spike binding assay to quantify the relative accumulation of sACE2 on the surface expressed spike protein **(Figure 4A**). After tagging sACE2 with superfolder GFP (sfGFP) we collected CM for each fusion protein and then incubated with spike expressing HEK293T cells (**Figure S5A**). Overlay images show that SunTag systems with either WT or v1, clearly enhanced the spike binding occupancy compared to their untagged partners (**Figure 4A**). Similar to earlier work, individual components of the SunTag system, sACE2-5xGCN4 and sACE2-scFvGCN4, did not demonstrate increased spike binding occupancy (**Figure S5B**). These data suggest that multiple sACE2 recruitment around spike proteins provides a much higher binding affinity. It would be interesting to increase the linker lengths and to use 10x or 24x versions of SunTag and examine if further enhancement in neutralization would be obtained.

As stability can be a major issue for protein-based drugs, we then tested the impact of storage at either 4ºC for 10 days or 37ºC for 24h on pseudovirus neutralization (**Figure S6A and S6B**). Although a slight decrease was observed in the neutralization efficiencies after long term storage, both WT-SunTag and v1-SunTag were more efficient than their untagged counterpart, demonstrating that these proteins could be amenable to current cold-chain logistics. Interestingly, the neutralization capacity of both monomeric and multimeric sACE2(v1) was more significantly affected than sACE2(WT) protein upon storage for 10 days at 4ºC (**Figure S6A**). One of the four point mutations found in sACE2(v1) (T92Q) disrupts a consensus glycosylation motif formed by N90 and T92 residues which may lower overall stability (28). This may also be the reason why bands of v1 variants were slightly lower in SDS-PAGE (**Figure 2B**). Therefore, using SunTag with other sACE2 variants (28, 30) protecting the glycosylation motifs may give a better stability, and even better neutralization efficiency.

On the other hand, using wild type sACE2 while keeping its enzymatic activity at maximum would have some therapeutic benefits by compensating disturbed ACE2 activity in lungs of infected patients (38). Moreover, a recent case report showed that sACE2 inhibited SARS-CoV-2 infection in a severe patient without interfering with the formation of neutralizing antibodies by the patient's immune system (32, 39). However, wild type sACE2 should be used in very high concentrations to achieve effective neutralization. Therefore, increasing sACE2 affinity to Spike via the SunTag system could be a promising strategy for COVID-19 treatment.

Using soluble decoy receptors is an attractive approach to treat SARS-CoV-2. While viruses can acquire escape mutations to monoclonal antibodies targeting viral proteins like Spike, host cellular receptors are unlikely to be affected by viral mutations. Therefore, decoy receptors can potentially overcome common forms of SARS-CoV-2 resistance including the novel variants (39). However, the initial sACE2 decoy receptors have been limited by relatively poor activity compared to monoclonal antibodies. In this work, we demonstrate that incorporating multiple sACE2 via a SunTag system can generate a decoy receptor that can effectively prevent SARS-CoV-2 cellular infection. With sACE2(WT), this multimeric decoy receptor was nearly 250-fold more active than the monomeric protein. Utilizing a mutant sACE2(v1), which has greater affinity for Spike, we could enhance the neutralization with our multimeric system to comparable levels as Spike monoclonal antibodies currently in clinical development. This proof-of-principle study utilized a

SunTag approach to generate multimeric decoy receptors but any alternative peptide-scFv couples could be incorporated with the ACE2. Overall, we believe that highly potent multimeric sACE2 decoy receptors are promising agents, which can be used as a treatment against COVID-19.

Acknowledgments

We thank Dr. Tamer Onder for critical comments on the manuscript. The authors acknowledge the financial support and use of the services and facilities of the Koç University Research Center for Translational Medicine (KUTTAM), funded by the Presidency of Turkey, Presidency of Strategy and Budget.

Author Contributions

Study design: AK, UA, DO and TBO; cloning: AK, UA, DO; pseudovirus production and neutralization: AK; protein purification: AK, ES and CA; SARS-CoV-2 isolation and neutralization: FC, OD, EN and BO; spike binding assay and IF staining: GNS, AK; supplied reagents and lines: NL, CA, MK, FC, and IS; data interpretation: AK, NL, IS and TBO; initial manuscript draft: AK, UA, DO and TBO; approved final manuscript: all authors.

Competing Interests

The authors declare no competing interests.

FIGURES:

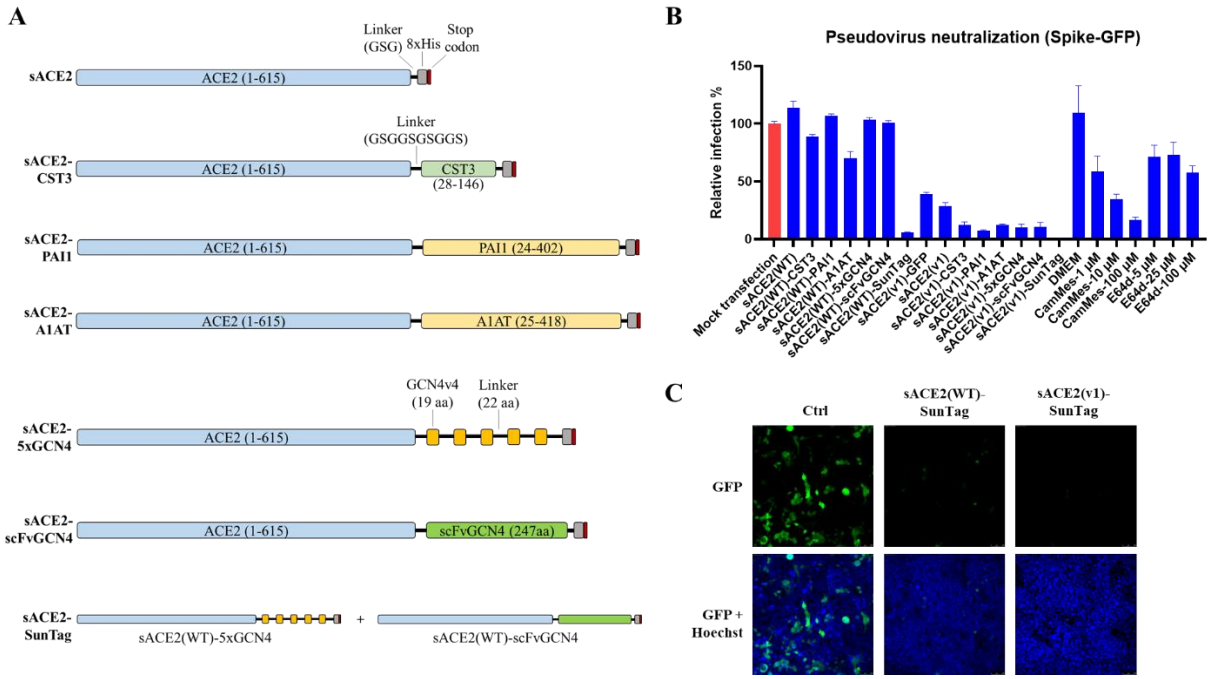

Figure 1. Pseudovirus neutralization screen with conditioned media of sACE2 fusions. A) Schematic representations of sACE2 fusions. **B)** Relative infection of ACE2 and TMPRSS2-expressing HEK293T cells with pseudoviruses bearing SARS-CoV-2 Spike in the presence of conditioned media (CM) collected from sACE2-expressing cells, or chemical inhibitors. CM from mock transfected cells were used as control (red bar), and infection rates were calculated as relative fluorescence to control wells. CamMes: Camostat Mesylate. **C)** Representative images of pseudovirus neutralization via sACE2(WT)-SunTag and sACE2(v1)-SunTag. Infected cells are green as they express GFP. Cell nuclei were stained with Hoechst 33342 dye.

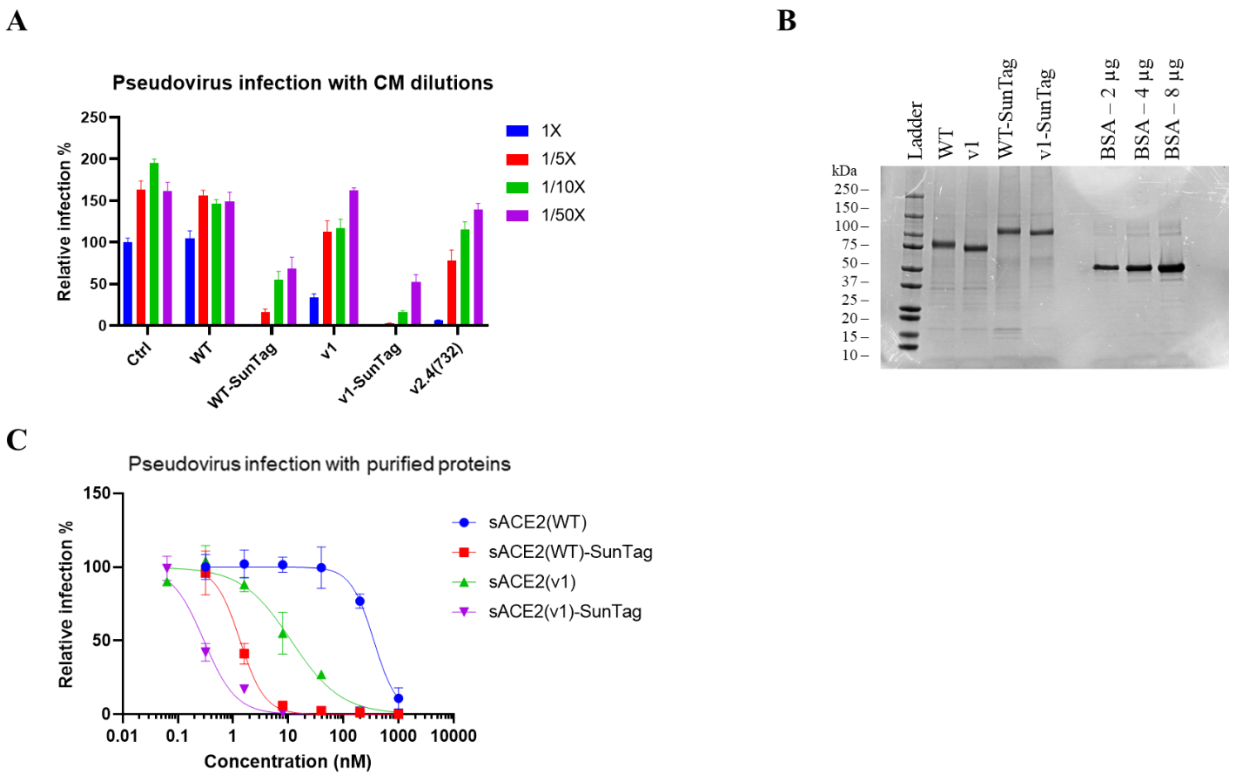

Figure 2. Pseudovirus neutralization with different concentrations of sACE2 constructs. A) Relative infection rate of ACE2 and TMPRSS2-expressing HEK293T cells with pseudoviruses bearing SARS-CoV-2 Spike in the presence of conditioned media (CM) collected from sACE2-expressing cells. CM were diluted with DMEM up to 1/50X. CM from mock transfected cells were used as control, and infection rates were calculated as relative fluorescence to control wells. **B)** SDS PAGE analysis of purified proteins. Protein ladder and different amounts of bovine serum albumin (BSA) were used as controls. **C)** Relative infection rate of ACE2 and TMPRSS2-expressing HEK293T cells with pseudoviruses bearing SARS-CoV-2 Spike in the presence of purified sACE2 proteins. Purified proteins were serially diluted in culture media. Culture medium was used as control, and infection rates were calculated as relative fluorescence to control wells.

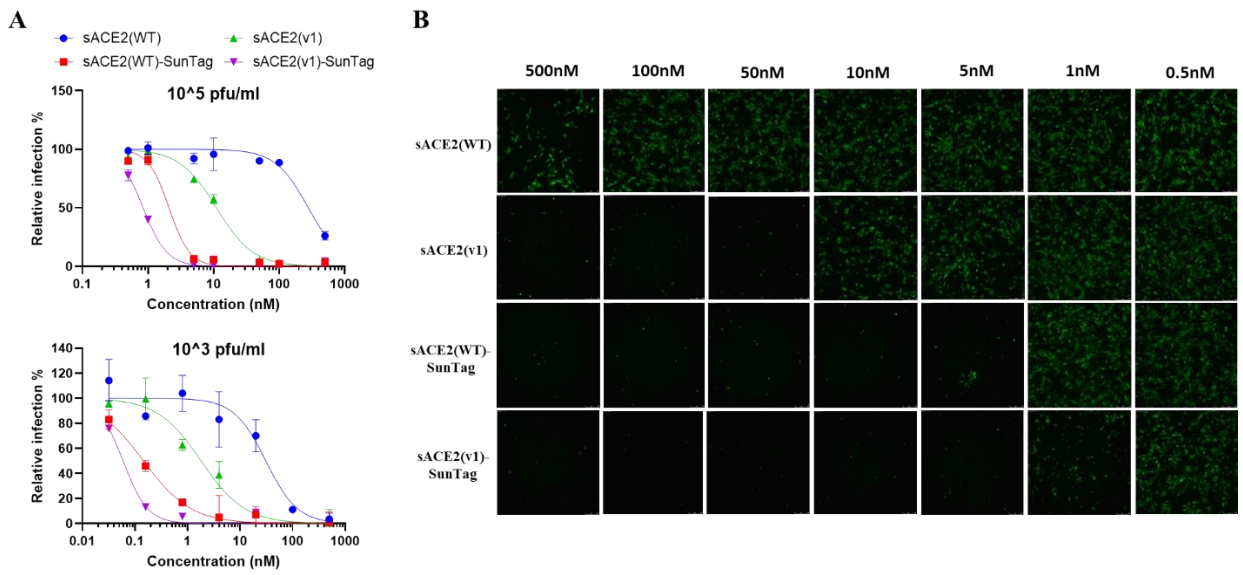

Figure 3. Neutralization assay with SARS-CoV-2 isolate. Relative infection of Vero-CCL81 cells with 10^5 pfu/ml **(A)** or 10^3 pfu/ml **(C)** SARS-CoV-2 isolate upon incubation with different concentrations of purified sACE2 proteins for 1h. Infection was measured by fluorescence measured upon immunostaining with anti-SARS-CoV-2 Spike primary antibody and Alexa Fluor-488 secondary antibody. **B)** Microscopic images of Vero-CCL81 cells infected with SARS-CoV-2 isolate (10^5 pfu/ml) upon incubation with different concentrations of purified sACE2 proteins for 1h. Cells were fixed after 24h of infection and immunostained with anti-SARS-CoV-2 Spike primary antibody and Alexa Fluor-488 secondary antibody.

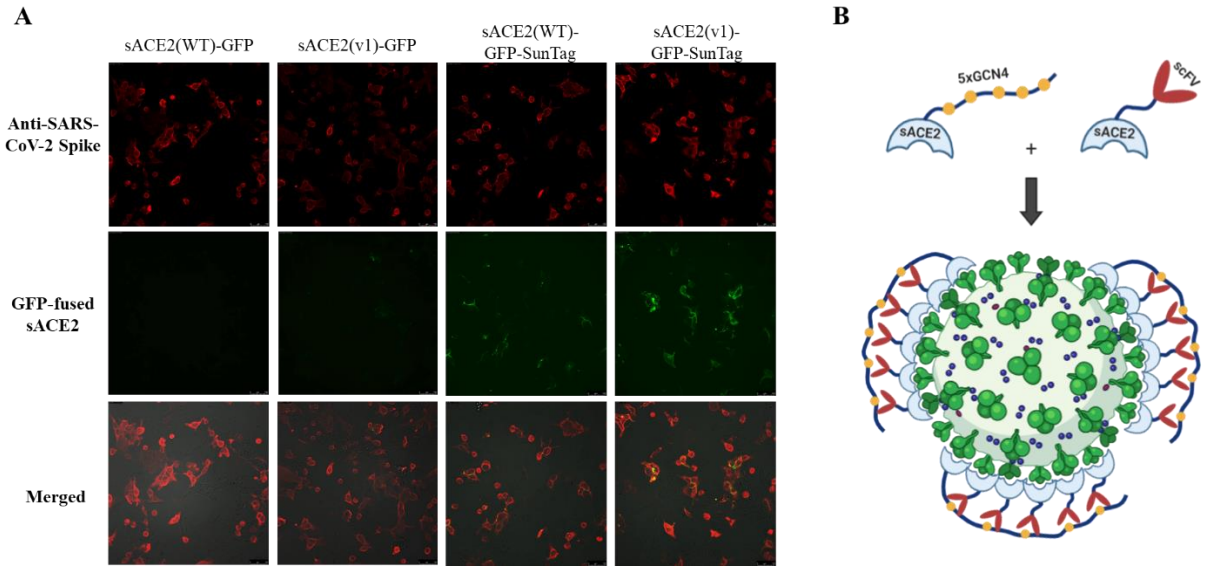

Figure 4. Spike-binding assay. A) HEK293T cells expressing SARS-CoV-2 Spike were incubated with conditioned media collected from GFP-fused sACE2-expressing cells for 8h. Fixed cells were immunostained with anti-SARS-CoV-2 primary antibody, and Alexa Fluor-594 secondary antibody. **B)** Representative model for binding of the SunTag system to SARS-CoV-2 virus.

References:

1. Coronaviridae Study Group of the International Committee on Taxonomy of Viruses, The species Severe acute respiratory syndrome-related coronavirus: classifying 2019-nCoV and naming it SARS-CoV-2. Nat Microbiol. 5, 536–544 (2020).

2. N. Zhu, D. Zhang, W. Wang, X. Li, B. Yang, J. Song, X. Zhao, B. Huang, W. Shi, R. Lu, P. Niu, F. Zhan, X. Ma, D. Wang, W. Xu, G. Wu, G. F. Gao, W. Tan, A Novel Coronavirus from Patients with Pneumonia in China, 2019. New England Journal of Medicine. 382 (2020), pp. 727–733.

3. WHO Director-General's opening remarks at the media briefing on COVID-19 - 11 March 2020, (available at https://www.who.int/director-general/speeches/detail/who-director-general-s-opening-remarks-at-the-media-briefing-on-covid-19---11-march-2020).

4. WHO Coronavirus Disease (COVID-19) Dashboard, (available at https://covid19.who.int).

5. N. Lurie, M. Saville, R. Hatchett, J. Halton, Developing Covid-19 Vaccines at Pandemic Speed. N. Engl. J. Med. 382, 1969–1973 (2020).

6. M. Voysey, S. A. C. Clemens, S. A. Madhi, L. Y. Weckx, P. M. Folegatti, P. K. Aley, B. Angus, V. L. Baillie, S. L. Barnabas, Q. E. Bhorat, S. Bibi, C. Briner, P. Cicconi, A. M. Collins, R. Colin-Jones, C. L. Cutland, T. C. Darton, K. Dheda, C. J. A. Duncan, K. R. W. Emary, K. J. Ewer, L. Fairlie, S. N. Faust, S. Feng, D. M. Ferreira, A. Finn, A. L. Goodman, C. M. Green, C. A. Green, P. T. Heath, C. Hill, H. Hill, I. Hirsch, S. H. C. Hodgson, A. Izu, S. Jackson, D. Jenkin, C. C. D. Joe, S. Kerridge, A. Koen, G. Kwatra, R. Lazarus, A. M. Lawrie, A. Lelliott, V. Libri, P. J. Lillie, R. Mallory, A. V. A. Mendes, E. P. Milan, A. M. Minassian, A. McGregor, H. Morrison, Y. F. Mujadidi, A. Nana, P. J. O'Reilly, S. D. Padayachee, A. Pittella, E. Plested, K. M. Pollock, M. N. Ramasamy, S. Rhead, A. V. Schwarzbold, N. Singh, A. Smith, R. Song, M. D. Snape, E. Sprinz, R. K. Sutherland, R. Tarrant, E. C. Thomson, M. E. Török, M. Toshner, D. P. J. Turner, J. Vekemans, T. L. Villafana, M. E. E. Watson, C. J. Williams, A. D. Douglas, A. V. S. Hill, T. Lambe, S. C. Gilbert, A. J. Pollard, Oxford COVID Vaccine Trial Group, Safety and efficacy of the ChAdOx1 nCoV-19 vaccine (AZD1222) against SARS-CoV-2: an interim analysis of four randomised controlled trials in Brazil, South Africa, and the UK. Lancet (2020), doi:10.1016/S0140-6736(20)32661-1.

7. L. R. Baden, H. M. El Sahly, B. Essink, K. Kotloff, S. Frey, R. Novak, D. Diemert, S. A. Spector, N. Rouphael, C. B. Creech, J. McGettigan, S. Kehtan, N. Segall, J. Solis, A. Brosz, C. Fierro, H. Schwartz, K. Neuzil, L. Corey, P. Gilbert, H. Janes, D. Follmann, M. Marovich, J. Mascola, L. Polakowski, J. Ledgerwood, B. S. Graham, H. Bennett, R. Pajon, C. Knightly, B. Leav, W. Deng, H. Zhou, S. Han, M. Ivarsson, J. Miller, T. Zaks, COVE Study Group, Efficacy and Safety of the mRNA-1273 SARS-CoV-2 Vaccine. N. Engl. J. Med. (2020), doi:10.1056/NEJMoa2035389.

8. F. P. Polack, S. J. Thomas, N. Kitchin, J. Absalon, A. Gurtman, S. Lockhart, J. L. Perez, G. Pérez Marc, E. D. Moreira, C. Zerbini, R. Bailey, K. A. Swanson, S. Roychoudhury, K. Koury, P. Li, W. V. Kalina, D. Cooper, R. W. Frenck Jr, L. L. Hammitt, Ö. Türeci, H. Nell, A. Schaefer, S. Ünal, D. B.

Tresnan, S. Mather, P. R. Dormitzer, U. Şahin, K. U. Jansen, W. C. Gruber, C4591001 Clinical Trial Group, Safety and Efficacy of the BNT162b2 mRNA Covid-19 Vaccine. N. Engl. J. Med. 383, 2603–2615 (2020).

9. E. Tchesnokov, J. Feng, D. Porter, M. Götte, Mechanism of Inhibition of Ebola Virus RNA-Dependent RNA Polymerase by Remdesivir. Viruses. 11 (2019), p. 326.

10. C. S. Kraft, Editorial Commentary: Considerations of Favipiravir as a Medical Countermeasure in Future Randomized Controlled Trials Against Ebola Virus Disease. Clinical Infectious Diseases. 63 (2016), pp. 1295–1296.

11. D. B. Shrestha, P. Budhathoki, S. Khadka, P. B. Shah, N. Pokharel, P. Rashmi, Favipiravir versus other antiviral or standard of care for COVID-19 treatment: a rapid systematic review and meta-analysis. Virol. J. 17, 141 (2020).

12. J. H. Beigel, K. M. Tomashek, L. E. Dodd, A. K. Mehta, B. S. Zingman, A. C. Kalil, E. Hohmann, H. Y. Chu, A. Luetkemeyer, S. Kline, D. Lopez de Castilla, R. W. Finberg, K. Dierberg, V. Tapson, L. Hsieh, T. F. Patterson, R. Paredes, D. A. Sweeney, W. R. Short, G. Touloumi, D. C. Lye, N. Ohmagari, M.-D. Oh, G. M. Ruiz-Palacios, T. Benfield, G. Fätkenheuer, M. G. Kortepeter, R. L. Atmar, C. B. Creech, J. Lundgren, A. G. Babiker, S. Pett, J. D. Neaton, T. H. Burgess, T. Bonnett, M. Green, M. Makowski, A. Osinusi, S. Nayak, H. C. Lane, ACTT-1 Study Group Members, Remdesivir for the Treatment of Covid-19 - Final Report. N. Engl. J. Med. 383, 1813–1826 (2020).

13. A. C. Walls, Y.-J. Park, M. A. Tortorici, A. Wall, A. T. McGuire, D. Veesler, Structure, Function, and Antigenicity of the SARS-CoV-2 Spike Glycoprotein. Cell. 183, 1735 (2020).

14. P. Zhou, X.-L. Yang, X.-G. Wang, B. Hu, L. Zhang, W. Zhang, H.-R. Si, Y. Zhu, B. Li, C.-L. Huang, H.-D. Chen, J. Chen, Y. Luo, H. Guo, R.-D. Jiang, M.-Q. Liu, Y. Chen, X.-R. Shen, X. Wang, X.-S. Zheng, K. Zhao, Q.-J. Chen, F. Deng, L.-L. Liu, B. Yan, F.-X. Zhan, Y.-Y. Wang, G.-F. Xiao, Z.-L. Shi, A pneumonia outbreak associated with a new coronavirus of probable bat origin. Nature. 579, 270–273 (2020).

15. Y. Wan, J. Shang, R. Graham, R. S. Baric, F. Li, Receptor Recognition by the Novel Coronavirus from Wuhan: an Analysis Based on Decade-Long Structural Studies of SARS Coronavirus. J. Virol. 94 (2020), doi:10.1128/JVI.00127-20.

16. D. Wrapp, N. Wang, K. S. Corbett, J. A. Goldsmith, C.-L. Hsieh, O. Abiona, B. S. Graham, J. S. McLellan, Cryo-EM Structure of the 2019-nCoV Spike in the Prefusion Conformation. bioRxiv (2020), doi:10.1101/2020.02.11.944462.

17. M. Hoffmann, H. Kleine-Weber, S. Schroeder, N. Krüger, T. Herrler, S. Erichsen, T. S. Schiergens, G. Herrler, N.-H. Wu, A. Nitsche, M. A. Müller, C. Drosten, S. Pöhlmann, SARS-CoV-2 Cell Entry Depends on ACE2 and TMPRSS2 and Is Blocked by a Clinically Proven Protease Inhibitor. Cell. 181, 271–280.e8 (2020).

18. M. Letko, A. Marzi, V. Munster, Functional assessment of cell entry and receptor usage for SARS-CoV-2 and other lineage B betacoronaviruses. Nat Microbiol. 5, 562–569 (2020).

19. P. Breining, A. L. Frølund, J. F. Højen, J. D. Gunst, N. B. Staerke, E. Saedder, M. Cases-Thomas, P. Little, L. P. Nielsen, O. S. Søgaard, M. Kjolby, Camostat mesylate against SARS-CoV-2 and COVID-19—Rationale, dosing and safety. Basic & Clinical Pharmacology & Toxicology (2020), doi:10.1111/bcpt.13533.

20. C. Wang, W. Li, D. Drabek, N. M. A. Okba, R. van Haperen, Albert D M, F. J. M. van Kuppeveld, B. L. Haagmans, F. Grosveld, B.-J. Bosch, A human monoclonal antibody blocking SARS-CoV-2 infection, doi:10.1101/2020.03.11.987958.

21. A. Z. Wec, D. Wrapp, A. S. Herbert, D. P. Maurer, D. Haslwanter, M. Sakharkar, R. K. Jangra, M. E. Dieterle, A. Lilov, D. Huang, L. V. Tse, N. V. Johnson, C.-L. Hsieh, N. Wang, J. H. Nett, E. Champney, I. Burnina, M. Brown, S. Lin, M. Sinclair, C. Johnson, S. Pudi, R. Bortz 3rd, A. S. Wirchnianski, E. Laudermilch, C. Florez, J. M. Fels, C. M. O'Brien, B. S. Graham, D. Nemazee, D. R. Burton, R. S. Baric, J. E. Voss, K. Chandran, J. M. Dye, J. S. McLellan, L. M. Walker, Broad neutralization of SARS-related viruses by human monoclonal antibodies. Science. 369, 731–736 (2020).

22. D. Pinto, Y.-J. Park, M. Beltramello, A. C. Walls, M. A. Tortorici, S. Bianchi, S. Jaconi, K. Culap, F. Zatta, A. De Marco, A. Peter, B. Guarino, R. Spreafico, E. Cameroni, J. B. Case, R. E. Chen, C. Havenar-Daughton, G. Snell, A. Telenti, H. W. Virgin, A. Lanzavecchia, M. S. Diamond, K. Fink, D. Veesler, D. Corti, Cross-neutralization of SARS-CoV-2 by a human monoclonal SARS-CoV antibody. Nature. 583, 290–295 (2020).

23. J. Hansen, A. Baum, K. E. Pascal, V. Russo, S. Giordano, E. Wloga, B. O. Fulton, Y. Yan, K. Koon, K. Patel, K. M. Chung, A. Hermann, E. Ullman, J. Cruz, A. Rafique, T. Huang, J. Fairhurst, C. Libertiny, M. Malbec, W.-Y. Lee, R. Welsh, G. Farr, S. Pennington, D. Deshpande, J. Cheng, A. Watty, P. Bouffard, R. Babb, N. Levenkova, C. Chen, B. Zhang, A. Romero Hernandez, K. Saotome, Y. Zhou, M. Franklin, S. Sivapalasingam, D. C. Lye, S. Weston, J. Logue, R. Haupt, M. Frieman, G. Chen, W. Olson, A. J. Murphy, N. Stahl, G. D. Yancopoulos, C. A. Kyratsous, Studies in humanized mice and convalescent humans yield a SARS-CoV-2 antibody cocktail. Science. 369, 1010–1014 (2020).

24. P. J. M. Brouwer, T. G. Caniels, K. van der Straten, J. L. Snitselaar, Y. Aldon, S. Bangaru, J. L. Torres, N. M. A. Okba, M. Claireaux, G. Kerster, A. E. H. Bentlage, M. M. van Haaren, D. Guerra, J. A. Burger, E. E. Schermer, K. D. Verheul, N. van der Velde, A. van der Kooi, J. van Schooten, M. J. van Breemen, T. P. L. Bijl, K. Sliepen, A. Aartse, R. Derking, I. Bontjer, N. A. Kootstra, W. J. Wiersinga, G. Vidarsson, B. L. Haagmans, A. B. Ward, G. J. de Bree, R. W. Sanders, M. J. van Gils, Potent neutralizing antibodies from COVID-19 patients define multiple targets of vulnerability. Science. 369, 643–650 (2020).

25. Y. Wu, F. Wang, C. Shen, W. Peng, D. Li, C. Zhao, Z. Li, S. Li, Y. Bi, Y. Yang, Y. Gong, H. Xiao, Z. Fan, S. Tan, G. Wu, W. Tan, X. Lu, C. Fan, Q. Wang, Y. Liu, C. Zhang, J. Qi, G. F. Gao, F.

Gao, L. Liu, A noncompeting pair of human neutralizing antibodies block COVID-19 virus binding to its receptor ACE2. Science. 368, 1274–1278 (2020).

26. Z. Liu, W. Xu, S. Xia, C. Gu, X. Wang, Q. Wang, J. Zhou, Y. Wu, X. Cai, D. Qu, T. Ying, Y. Xie, L. Lu, Z. Yuan, S. Jiang, RBD-Fc-based COVID-19 vaccine candidate induces highly potent SARS-CoV-2 neutralizing antibody response. Signal Transduct Target Ther. 5, 282 (2020).

27. E. Andreano, G. Piccini, D. Licastro, L. Casalino, N. V. Johnson, I. Paciello, S. D. Monego, E. Pantano, N. Manganaro, A. Manenti, R. Manna, E. Casa, I. Hyseni, L. Benincasa, E. Montomoli, R. E. Amaro, J. S. McLellan, R. Rappuoli, SARS-CoV-2 escape in vitro from a highly neutralizing COVID-19 convalescent plasma, doi:10.1101/2020.12.28.424451.

28. K. K. Chan, D. Dorosky, P. Sharma, S. A. Abbasi, J. M. Dye, D. M. Kranz, A. S. Herbert, E. Procko, Engineering human ACE2 to optimize binding to the spike protein of SARS coronavirus 2. Science. 369, 1261–1265 (2020).

29. L. Guo, W. Bi, X. Wang, W. Xu, R. Yan, Y. Zhang, K. Zhao, Y. Li, M. Zhang, X. Cai, S. Jiang, Y. Xie, Q. Zhou, L. Lu, B. Dang. Engineered trimeric ACE2 binds viral spike protein and locks it in "Three-up" conformation to potently inhibit SARS-CoV-2 infection. Cell Research (2020), doi:10.1038/s41422-020-00438-w.

30. A. Glasgow, J. Glasgow, D. Limonta, P. Solomon, I. Lui, Y. Zhang, M. A. Nix, N. J. Rettko, S. Zha, R. Yamin, K. Kao, O. S. Rosenberg, J. V. Ravetch, A. P. Wiita, K. K. Leung, S. A. Lim, X. X. Zhou, T. C. Hobman, T. Kortemme, J. A. Wells, Engineered ACE2 receptor traps potently neutralize SARS-CoV-2. Proc. Natl. Acad. Sci. U. S. A. 117, 28046–28055 (2020).

31. V. Monteil, H. Kwon, P. Prado, A. Hagelkrüys, R. A. Wimmer, M. Stahl, A. Leopoldi, E. Garreta, C. Hurtado Del Pozo, F. Prosper, J. P. Romero, G. Wirnsberger, H. Zhang, A. S. Slutsky, R. Conder, N. Montserrat, A. Mirazimi, J. M. Penninger, Inhibition of SARS-CoV-2 Infections in Engineered Human Tissues Using Clinical-Grade Soluble Human ACE2. Cell. 181, 905–913.e7 (2020).

32. A. Zoufaly, M. Poglitsch, J. H. Aberle, W. Hoepler, T. Seitz, M. Traugott, A. Grieb, E. Pawelka, H. Laferl, C. Wenisch, S. Neuhold, D. Haider, K. Stiasny, A. Bergthaler, E. Puchhammer-Stoeckl, A. Mirazimi, N. Montserrat, H. Zhang, A. S. Slutsky, J. M. Penninger, Human recombinant soluble ACE2 in severe COVID-19. The Lancet Respiratory Medicine. 8 (2020), pp. 1154–1158.

33. M. Dittmann, H.-H. Hoffmann, M. A. Scull, R. H. Gilmore, K. L. Bell, M. Ciancanelli, S. J. Wilson, S. Crotta, Y. Yu, B. Flatley, J. W. Xiao, J.-L. Casanova, A. Wack, P. D. Bieniasz, C. M. Rice, A serpin shapes the extracellular environment to prevent influenza A virus maturation. Cell. 160, 631–643 (2015).

34. C. C. Tseng, C. P. Tseng, M. J. Levine, L. A. Bobek, Differential effect toward inhibition of papain and cathepsin C by recombinant human salivary cystatin SN and its variants produced by a baculovirus system. Arch. Biochem. Biophys. 380, 133–140 (2000).

35. A. Baron, A. DeCarlo, J. Featherstone, Functional aspects of the human salivary cystatins in the oral environment. Oral Dis. 5, 234–240 (1999).

36. M. E. Tanenbaum, L. A. Gilbert, L. S. Qi, J. S. Weissman, R. D. Vale, A protein-tagging system for signal amplification in gene expression and fluorescence imaging. Cell. 159, 635–646 (2014).

37. X. Xu, Y. Tao, X. Gao, L. Zhang, X. Li, W. Zou, K. Ruan, F. Wang, G.-L. Xu, R. Hu, A CRISPR-based approach for targeted DNA demethylation. Cell Discov. 2, 16009 (2016).

38. H. Zhang, J. M. Penninger, Y. Li, N. Zhong, A. S. Slutsky, Angiotensin-converting enzyme 2 (ACE2) as a SARS-CoV-2 receptor: molecular mechanisms and potential therapeutic target. Intensive Care Med. 46, 586–590 (2020).

39. WHO | SARS-CoV-2 Variants (2020) (available at http://www.who.int/csr/don/31-december-2020-sars-cov2-variants/en/).